

Research Article

Evaluation of Tropospheric and Ionospheric Effects on the Geographic Localization of Data Collection Platforms

C. C. Celestino, C. T. Sousa, W. Yamaguti, and H. K. Kuga

Received 29 September 2006; Accepted 23 April 2007

Recommended by José Manoel Balthazar

The Brazilian National Institute for Space Research (INPE) is operating the Brazilian Environmental Data Collection System that currently amounts to a user community of around 100 organizations and more than 700 data collection platforms installed in Brazil. This system uses the SCD-1, SCD-2, and CBERS-2 low Earth orbit satellites to accomplish the data collection services. The main system applications are hydrology, meteorology, oceanography, water quality, and others. One of the functionalities offered by this system is the geographic localization of the data collection platforms by using Doppler shifts and a batch estimator based on least-squares technique. There is a growing demand to improve the quality of the geographical location of data collection platforms for animal tracking. This work presents an evaluation of the ionospheric and tropospheric effects on the Brazilian Environmental Data Collection System transmitter geographic location. Some models of the ionosphere and troposphere are presented to simulate their impacts and to evaluate performance of the platform location algorithm. The results of the Doppler shift measurements, using the SCD-2 satellite and the data collection platform (DCP) located in Cuiabá town, are presented and discussed.

Copyright © 2007 C. C. Celestino et al. This is an open access article distributed under the Creative Commons Attribution License, which permits unrestricted use, distribution, and reproduction in any medium, provided the original work is properly cited.

1. Introduction

The current Brazilian Environmental Data Collection System is composed of the SCD-1, SCD-2, and CBERS-2 satellite constellations (space segment), a network of more than 700 data collection platforms (DCP) spread out in Brazil, the Reception Stations of Cuiabá and Alcântara, and the Data Collection Mission Center. Figure 1.1(a) illustrates the Brazilian Environmental Data Collection System and Figure 1.1(b) the system space segment. In this system, the satellite works as a message retransmitter (bent pipe transponder).

2 Mathematical Problems in Engineering

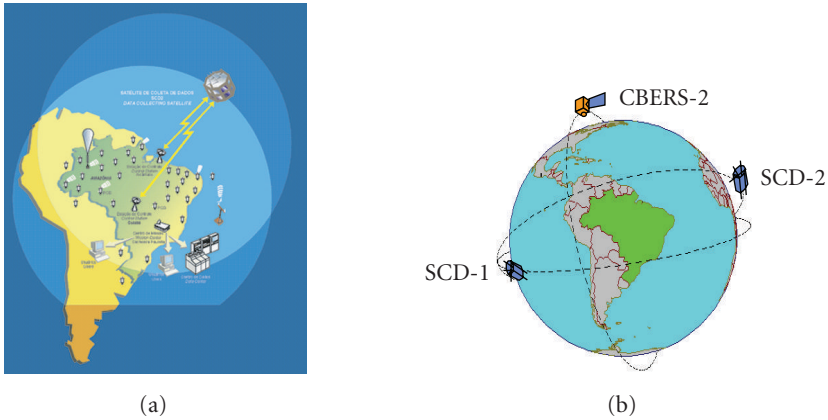


Figure 1.1. (a) Brazilian Environmental Data Collection System with Cuiabá and Alcântara station visibility circles and (b) space segment composed of SCD-1, SCD-2, and CBERS-2 satellites.

A communication link between a data collection platform (DCP) and a reception station is established through one of the satellites. The platforms installed on ground (fixed or mobile) are configured for transmission intervals spanning from 40 to 220 seconds. Each message may have up to 32 bytes of useful data that correspond to a 1-second transmission burst. The DCP messages retransmitted by the satellites and received by the Cuiabá or Alcântara stations are sent to the Data Collection Mission Center located at Cachoeira Paulista (São Paulo state) for processing, storage, and dissemination to the users. The users receive the processed data through Internet, at most 30 minutes after being received at a station. The DCP geographical location could be determined by using the Doppler effect or by the use of a GPS receiver. Considering the Doppler shift as the platform location method, the coordinates of a platform are obtained from the Doppler shift measurements of the transmitter frequency carrier signal [1]. As these signals spread in the terrestrial atmosphere, among other factors, they are influenced by the electrochemical elements that compose the atmosphere layers, which generate a propagation delay, and cause errors in the final coordinates supplied to the system users. The signal propagation delay due to the atmospheric effects consists, essentially, of the ionospheric and tropospheric effects.

Zenithal delays due to ionosphere can range from a few meters up to dozens of meters, while that due to troposphere is usually around three meters [2]. To evaluate the impacts on geographical location due to the ionospheric and tropospheric effects, the SCD-2 satellite and DCP #32590, located in Cuiabá, with latitude 15.55293°S and longitude 56.06875°W were considered in this work.

The content of this article is the following: the effects in the geographic location and characteristics of the ionosphere and troposphere are shown in Section 2; the models are described in Section 3; in Section 4, qualitative analyses of the ionospheric and tropospheric effects are presented; Section 5 presents the results of the evaluation of tropospheric and ionospheric effects, and Section 6 presents the conclusions and final remarks.

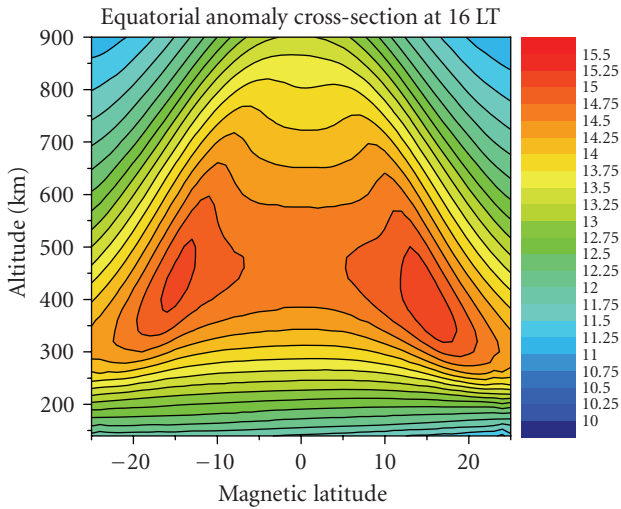


Figure 2.1. Ionospheric electron density (expressed as \ln in units of cm^{-3}) in the magnetic meridional plane for the Brazilian longitudinal sector calculated by Sheffield University Plasmasphere Ionosphere Model (Communication: Jonas R. Souza and G. J. Bailey).

2. Ionosphere and troposphere characteristics

This section presents a brief description of the ionosphere and troposphere characteristics.

2.1. Ionosphere. The ionosphere layer is located between 50 and 1.000 kilometers above the Earth surface [3], and is composed of ions and electrons, being thus named ionosphere. The key agent of ionization is the Sun, whose radiation in the X-ray and ultraviolet bands inserts a great amount of free electrons in the environment. In the ionosphere the density of free electrons is variable in close connection with the hour of the day, season, and chemical composition of the high atmosphere. The refraction in the ionosphere depends on the signal frequency and is proportional to the total electron content (TEC) along the path traveled by the signal between platform and satellite.

Figure 2.1 shows a sample of the ionospheric electron density. The data of the ionosphere in Brazil are obtained using rockets, satellites, modeling systems, and simulation of the ionospheric and thermospheric processes.

2.2. Troposphere. The effect of the troposphere depends on the density of the atmosphere and on the satellite line of sight elevation angle. This effect can be observed from ground up to approximately 50 km height. Tropospheric effect on signal propagation at frequencies below 30 GHz do not depend on the transmitted frequency [3]. The influence of the gaseous mass can be divided in two parts: (a) composed of dry gases, called dry or hydrostatic component and, (b) composed of water vapor, called wet or humid component. The tropospheric delay is generated by these components: hydrostatic and

4 Mathematical Problems in Engineering

wet. The delay due to hydrostatic component can correspond to approximately 2 to 3 m in the zenith and it varies with the temperature and the local atmospheric pressure [3]; the delay for the wet component is of approximately 1 to 30 cm at the zenith [4], however its variation is very large. Its prediction with good accuracy becomes a difficult task.

3. Ionospheric and tropospheric models

The models used in this work are described below.

3.1. Ionospheric model. The ionospheric signal delay is given by [5]

$$R_I = \frac{40.3 \text{ VTEC sec } Z}{f^2}, \quad (3.1)$$

where VTEC is the total electron content in the vertical direction (el/m^2), Z is the signal path zenithal angle in relation to the plane of the mean altitude of 350 km approximately, and f is the platform transmitter frequency (Hz).

At the ionospheric pierce point Z is given as

$$\sin Z = \frac{R_E \cos \gamma}{R_E + H}, \quad (3.2)$$

where R_E is the Earth's equatorial radius, H and γ are altitude and satellite elevation angle, respectively.

Substituting (3.2) in (3.1) and differentiating in function to time, we get

$$\dot{R}_I = -\frac{36.2 \text{ VTEC } \cos \gamma \sin \gamma \dot{\gamma}}{f^2 (1 - 0.9 \cos^2 \gamma)^{3/2}}, \quad (3.3)$$

where $\dot{\gamma}$ is satellite elevation angle rate.

Equation (3.1) models the ionospheric signal delay and (3.3) models the time variation of this delay. This can be applied to the ionospheric correction based on the Doppler shift measurements.

The delay due to the ionosphere is sensitive to the variable VTEC. The values used for this variable were obtained from IRI-2001 (International Reference Ionosphere) [6].

3.2. Tropospheric models. Three tropospheric models are considered. The first model is the Hopfield empiric model for the tropospheric delay in function of the temperature and pressure values measured on ground. It is given by [4]

$$T_r^s = T_{ZH} m_b(\gamma) + T_{ZW} m_w(\gamma), \quad (3.4)$$

where

$$T_{ZH} = 155.2 \times 10^{-7} \frac{P}{T} H_d \quad (3.5)$$

is the zenithal delay of the dry component,

$$T_{ZW} = 155.2 \times 10^{-7} \frac{4810e}{T^2} H_W \quad (3.6)$$

is the zenithal delay of the humid component, T is the temperature (in degrees K), P is the dry pressure (in hPa), e is the humid pressure (in hPa), and

$$\begin{aligned} H_d &= 40136 + 148.72(T - 273.16), \\ H_W &= 11000\text{m}. \end{aligned} \quad (3.7)$$

$m_b(\gamma)$ and $m_w(\gamma)$ are mapping functions that relate the dry and humid delay components with the elevation angle (γ) in degrees and are given by

$$\begin{aligned} m_b(\gamma) &= \csc(\gamma^2 + 6.25)^{1/2}, \\ m_w(\gamma) &= \csc(\gamma^2 + 2.25)^{1/2}. \end{aligned} \quad (3.8)$$

The second model is the Saastamoinen model [7–9]:

$$\begin{aligned} T_{ZH} &= 0.002277DP, \\ T_{ZW} &= 0.002277eD \left(\frac{1255}{T} + 0.05 \right), \end{aligned} \quad (3.9)$$

where $D = (1 + 0.0026 \cos 2\varphi + 0.00028H)$, and φ and H (in km) are the satellite latitude and altitude, respectively.

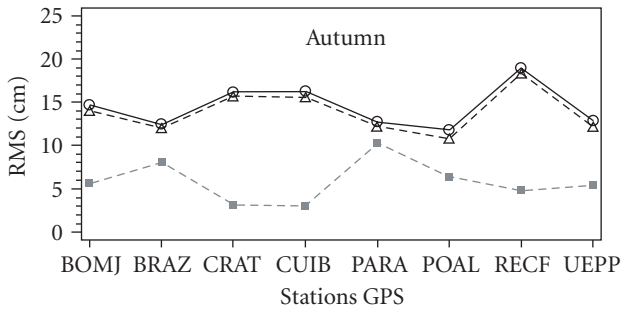
The third model is a dynamic model that is being used at Center for Weather Forecasting and Climate Studies (CPTEC-INPE) to provide the zenithal tropospheric delay (Z_{TD}). The predictions of Z_{TD} values are obtained from estimation of temperature, surface atmospheric pressure and humidity generated by the numeric weather prediction (NWP) with observed initial conditions [10]. The dynamic model data are available on the Internet site <http://satelite.cptec.inpe.br/htmldocs/ztd/zenital.htm>.

4. Qualitative analysis of the ionospheric and tropospheric effects

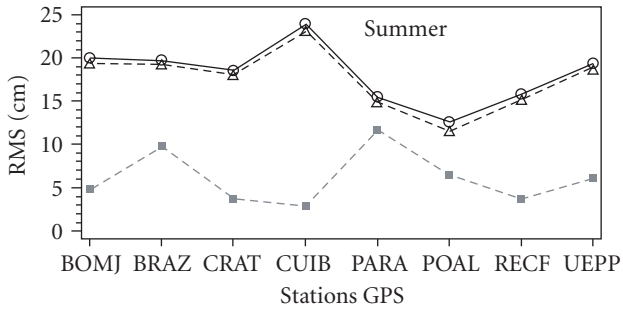
This section presents a qualitative analysis of the tropospheric delay values (hydrostatic and wet components) using the CPTEC's dynamic model [10] and the ionospheric delay values obtained from the IRI's model [6].

Figure 4.1 shows the root mean square (RMS) errors of the zenithal tropospheric delay resulted from comparison between the dynamic modeling of [10], the Hopfield empiric

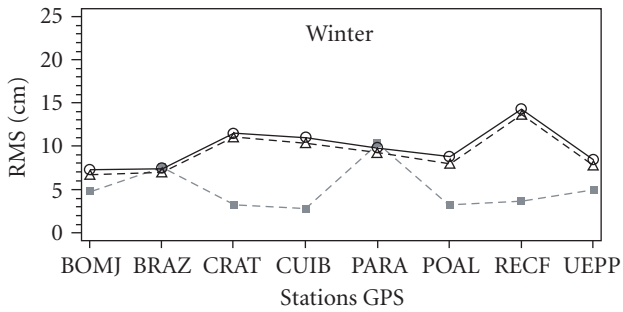
6 Mathematical Problems in Engineering



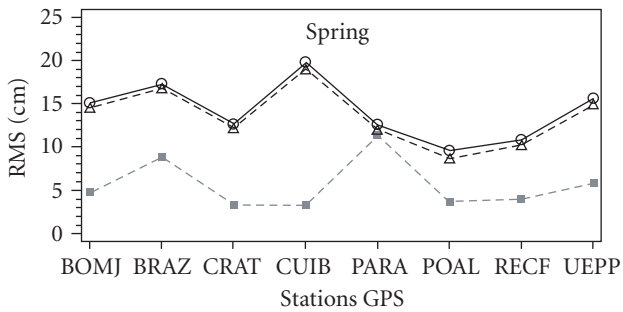
(a)



(b)



(c)



(d)

Figure 4.1. Zenithal tropospheric delay RMS values resulted from comparison of Hopfield (\circ), Saastamoinen (\triangle), dynamic (\blacksquare) models, and GPS reference data (source: [10]).

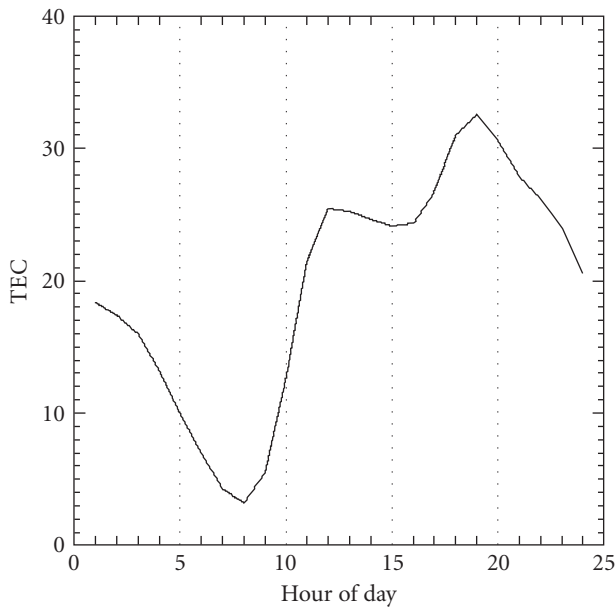


Figure 4.2. VTEC values for DCP no. 32590 location (IRI-2001).

model [4], the Saastamoinen model [7–9], and GPS reference data from Brazilian Continuous GPS Network (RBMC) collected during one year starting from March 2004. Observe that the maximum RMS difference between the zenithal values is 20 cm approximately, considering the summer season and the GPS ground station in Cuiabá. This difference happens because in the Hopfield and Saastamoinen models mean values are used for the temperature, hydrostatic, and wet components while in the dynamic modeling the temperature is a real measurement. Besides, the Hopfield and Saastamoinen models standard mean values are obtained in the subtropical areas such as Europe and North America. For those reasons, the evaluation of the tropospheric effects in this work considers the data from dynamic modeling because it is more suitable for tropical conditions of Brazil.

Figure 4.2 shows the VTEC values used in the numeric simulations (IRI, 2001). These values were obtained considering the location of the 32590 DCP on 2006, April 7th. Observe that in this figure the largest value occurs at 7 pm UTC. The location errors due to this effect for 11 am and 6 pm were of 24.6 m and 39.5 m, respectively, as presented in Table 4.1.

In [11], the ionospheric zenithal signal delay considering Rio de Janeiro city (Brazil) is 30 meters approximately, and using the model IRI is 10 meters approximately. This difference happens because TEC causes a decrease in the GPS signal, and in the region above Brazil it depends strongly on the ionospheric equatorial anomaly [11]. For tropical regions like in Brazil, ionospheric irregularities occurrence can affect drastically the GPS performance.

Table 4.1. Geographical location errors considering DCP no. 32590 as obtained with simulated conditions, simulated location error due to ionospheric effect, simulated location error due to tropospheric effect, and simulated location error considering both effects.

Date UTC Time	Min elevation angle (deg)	Max elevation angle (deg)	Simulated location error (km)	Simulated ionospheric effect error (km)	Simulated tropospheric effect error (km)	Simulated location error with both effects (km)
April, 6 2 pm	4	27	0.0063	0.1296	0.0304	0.1628
April, 7 11 am	15	42	0.0154	0.1455	0.0304	0.1910
April, 7 6 pm	9	33	0.0063	0.1874	0.0399	0.2267
April, 10 9 am	10	73	0.0503	0.0545	0.0789	0.1835

The IRI ionospheric model results were used in this work for the DCP location. Knowing that the model can also be inaccurate, we can conclude that the location error due to the ionospheric effect can be larger than the values presented here.

5. Results

The results and analysis of the data collection platform geographic location due to the ionospheric and the tropospheric effects are shown here, demonstrating the location accuracy achieved. We obtained data collected in Cuiabá Reception Station (Central Brazil) using the Brazilian satellite SCD-2 of low orbit with 25° inclination in relation to Equator and altitude of approximately 750 km. We considered a nearby Data Collecting Platform number 32 590 with known latitude of 15.55293°S and longitude of 56.06875°W. We gathered representative data sets of 32 590 DCP transmitter at three different days and times as shown in Tables 4.1 and 5.1.

Table 4.1 shows the results considering simulated SCD2 Doppler shift values, representing simulated conditions. Table 5.1 shows the results from another analysis considering data measurements gathered in actual conditions.

The minimum elevation (γ_{\min}) and the maximum elevation (γ_{\max}) angles of the transmitted beam from the platform to satellite are presented in the second and third columns. We used the geographical location algorithm [1] to generate the results. The geographical location errors without considering ionospheric and tropospheric effects, simulated conditions, (e) are represented in the fourth column. The last three columns show location error results considering ionospheric effect ($e(\dot{R}_I)$), tropospheric effect ($e(\dot{R}_T)$), and both effects ($e(\dot{R}_I, \dot{R}_T)$) in the simulated Doppler shift measurements.

It can be observed in Table 4.1 that the error in DCP location in the simulated Doppler measurements due to the ionospheric effect was larger than the error considering the

Table 5.1. Geographical location errors for the DCP no. 32590 as obtained today without any correction (actual conditions), actual location error with ionospheric correction, actual location error with tropospheric correction, and final location error considering both corrections.

Date UTC Time	Min elevation angle (deg)	Max elevation angle (deg)	Actual location error (km)	Actual location error with ionospheric correction (km)	Actual location error with tropospheric correction (km)	Actual location error with both corrections (km)
April, 6 2 pm	11	27	0.35	0.25	0.33	0.24
April, 7 11 am	15	42	1.06	0.90	1.01	0.87
April, 7 6 pm	9	33	1.75	1.98	1.86	2.10
April, 10 9 am	10	73	2.17	1.87	1.74	1.47

tropospheric effect as expected. The maximum error in the observed location was 187 m for the ionospheric effect and the minimum error was 30 m for tropospheric effect.

Now considering actual conditions with data obtained from flying satellites as shown in Table 5.1, we can observe that in most cases the location error decreases when we consider both corrections as shown in the last column as expected. For these test cases, the errors decreased more than 100 m.

In Table 5.1, several visual inspections of the results generated for the actual case were made. In the first pass (April 6, 2 pm) it was observed that when eliminating the measurement with elevation below 10 degrees, the result was consistent with the expectations. Unlikely the introduction of this measurement in the total of 6 measurements worsened the final result.

Already in the third pass (April 7, 6 pm) two measurements were taken with elevation smaller than 10 degrees, remaining only two good measurements in the total of 4 measurements. With this, the final result was inconsistent with the expected result.

6. Conclusions

The performance analysis of the geographic location of data collection platforms considering the ionospheric and the tropospheric effects is shown. Two different analyses were made: in the first analysis results were obtained considering simulated Doppler shift of the SCD2 satellite pass, as representative of ideal conditions, and the total incremental error in the observed location was less than 227 m; in the second analysis, with data files depicting actual conditions, we can observe that in most cases the location error decreases around hundred meters. The April 7, 6 pm case (Table 5.1) presented insufficient data and its result was not considered representative.

On the average, for these tested cases, we can conclude that the location errors decreased when including the ionospheric and tropospheric corrections.

In as much as the location accuracy being a function of several factors such as on board oscillator stability, DCP transmitter oscillator stability, satellite orbital elements accuracy, data collection processing equipment performance, number of reception stations, among others, the correction of the effects of signal propagation through the ionosphere and troposphere can be an important factor to be considered.

The results herein indicate that the correction of the ionospheric and tropospheric effects can reduce the geographical location errors and improve the performance of the geographical location software.

A proposed follow-on research is to analyze in detail the ionospheric and tropospheric effects considering several DCPs located in different regions, as well as the year season to verify the impact of seasonal effects in the performance of the system. Furthermore, other models such as IONEX from IGS, and other mapping functions are being considered to be included in the system.

Acknowledgments

The authors thank the following people that contributed to this work: Mr. Luiz Fernando Sapucci (INPE) for supplying the tropospheric dynamic model data; Dr. Eurico R. de Paula (INPE) for the usage of IRI model; and to CNPq (Grant no. 382746/2005-8) and to FAPESP (Grant no. 2005/04497-0) for the financial support.

References

- [1] C. T. Sousa, "Geolocalização de Transmissores com Satélites Usando Desvio Doppler em Tempo Quase Real," Ph.D. dissertation, Space Engineering and Technology, Space Mechanics and Control Division, INPE-Instituto Nacional de Pesquisas Espaciais, São José dos Campos, Brazil, 2000.
- [2] J. A. Klobuchar, "Ionospheric effects on GPS," in *Global Positioning System: Theory and Applications*, B. W. Parkinson and J. J. Spilker Jr., Eds., vol. 1, pp. 485–515, American Institute of Aeronautics and Astronautics, Washington, DC, USA, 1996.
- [3] J. F. G. Mônico, *Posicionamento pelo NAVSTAR-GPS: Descrição, Fundamentos e Aplicações*, Unesp, São Paulo, Brazil, 2000.
- [4] G. Seeber, *Satellite Geodesy: Foundations, Methods, and Applications*, Walter de Gruyter, Berlin, Germany, 1993.
- [5] K. Aksnes, P. H. Andersen, and E. Haugen, "A precise multipass method for satellite Doppler positioning," *Celestial Mechanics*, vol. 44, no. 4, pp. 317–338, 1988.
- [6] D. Bilitza, International Reference Ionospheric Model—IRI, 2000 e 2001, <http://modelweb.gsfc.nasa.gov/models/iri.html>.
- [7] J. Saastamoinen, "Contribution to the theory of atmospheric refraction," *Bulletin Geodésique*, vol. 105, pp. 279–298, 1972.
- [8] J. Saastamoinen, "Contribution to the theory of atmospheric refraction," *Bulletin Geodésique*, vol. 106, pp. 383–397, 1972.
- [9] J. Saastamoinen, "Contribution to the theory of atmospheric refraction," *Bulletin Geodésique*, vol. 107, pp. 13–34, 1972.

- [10] L. F. Sapucci, L. A. T. Machado, and J. F. G. Mônico, "Predictions of Tropospheric Zenithal Delay for South America: Seasonal Variability and Quality Evaluation," *Revista Brasileira de Cartografia*. In press. 2007.
- [11] E. R. de Paula, I. J. Kantor, and L. F. C. de Rezende, "Characteristics of the GPS signal scintillations during ionospheric irregularities and their effects over the GPS system," in *Proceedings of the 4th Brazilian Symposium on Inertial Engineering (SBEIN '04)*, São José dos Campos, Brazil, November 2004.

C. C. Celestino: Division of Space Systems (DSE), National Institute for Space Research (INPE), 12227-010 São José dos Campos, Brazil
Email address: claudia@dss.inpe.br

C. T. Sousa: Mathematics Department, DMA-FEG-UNESP, CP 205, 12500-000 Guaratinguetá, Brazil
Email address: cristina@dss.inpe.br

W. Yamaguti: Division of Space Systems (DSE), National Institute for Space Research (INPE), 12227-010 São José dos Campos, Brazil
Email address: yamaguti@dss.inpe.br

H. K. Kuga: Division of Space Mechanics and Control (DMC), National Institute for Space Research (INPE), 12227-010 São José dos Campos, Brazil
Email address: hkk@dem.inpe.br